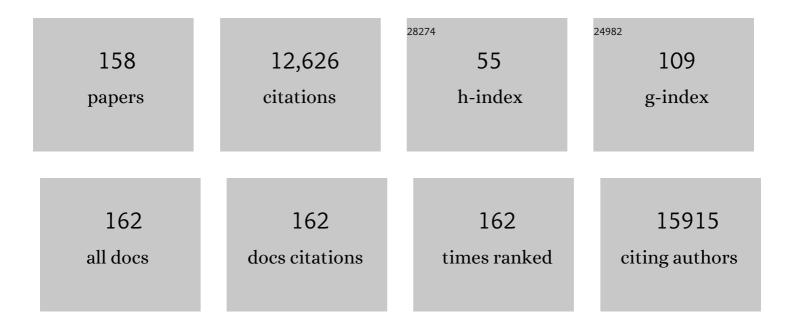
List of Publications by Year in descending order

Source: https://exaly.com/author-pdf/2986166/publications.pdf Version: 2024-02-01



ΗλΟΙΙΑΝΟ

#	Article	IF	CITATIONS
1	Isolated ultrasmall Bi nanosheets for efficient CO2-to-formate electroreduction. Nano Research, 2022, 15, 1409-1414.	10.4	26
2	Heterogeneous MoSe <sub>2</sub> /Nitrogenâ€Dopedâ€Carbon Nanoarrays: Engineering Atomic Interface for Potassiumâ€ion Storage. Advanced Functional Materials, 2022, 32, 2110223.	14.9	29
3	Regulating Steric Hindrance in Redoxâ€Active Porous Organic Frameworks Achieves Enhanced Sodium Storage Performance. Small, 2022, 18, e2105927.	10.0	10
4	Engineering V <sub>2</sub> O <sub>3</sub> nanoarrays with abundant localized defects towards high-voltage aqueous supercapacitors. Journal of Materials Chemistry A, 2022, 10, 4825-4832.	10.3	6
5	A New Design Method of Shield Tunnel Based on the Concept of Minimum Bending Moment. Applied Sciences (Switzerland), 2022, 12, 1082.	2.5	4
6	Defect engineered SnO <sub>2</sub> nanoparticles enable strong CO <sub>2</sub> chemisorption toward efficient electroconversion to formate. Dalton Transactions, 2022, 51, 3512-3519.	3.3	7
7	Low full-cell voltage driven high-current-density selective paired formate electrosynthesis. Journal of Materials Chemistry A, 2022, 10, 1329-1335.	10.3	18
8	Regulating Steric Hindrance in Redoxâ€Active Porous Organic Frameworks Achieves Enhanced Sodium Storage Performance (Small 1/2022). Small, 2022, 18, 2270004.	10.0	2
9	Co <sub>3</sub> O <sub>4</sub> Quantum Dot-Catalyzed Lithium Oxalate as a Capacity and Cycle-Life Enhancer in Lithium-Ion Full Cells. ACS Applied Energy Materials, 2022, 5, 2112-2120.	5.1	10
10	Enhancing Surface and Crystal Stability of the Ni-High NCA Cathode for High-Energy and Durable Lithium-Ion Batteries. Industrial & Engineering Chemistry Research, 2022, 61, 2817-2824.	3.7	10
11	Dual Rate-Modulation Approach for the Preparation of Crystalline Covalent Triazine Frameworks Displaying Efficient Sodium Storage. ACS Macro Letters, 2022, 11, 60-65.	4.8	12
12	Electricity generation from water evaporation through highly conductive carbonized wood with abundant hydroxyls. Sustainable Energy and Fuels, 2022, 6, 2249-2255.	4.9	11
13	Redox-mediated electrosynthesis of ethylene oxide from CO2 and water. Nature Catalysis, 2022, 5, 185-192.	34.4	40
14	Algorithm for an Effective Ratio of the Transverse Bending Rigidity Based on the Segment Joint Bending Stiffness. Applied Sciences (Switzerland), 2022, 12, 1901.	2.5	6
15	Introducing the Solvent Coâ€Intercalation Mechanism for Hard Carbon with Ultrafast Sodium Storage. Small, 2022, 18, e2108092.	10.0	14
16	Aluminum nanoparticles deliver a dual-epitope peptide for enhanced anti-tumor immunotherapy. Journal of Controlled Release, 2022, 344, 134-146.	9.9	21
17	Toward Highâ€Performance CO <sub>2</sub> â€ŧoâ€C <sub>2</sub> Electroreduction via Linker Tuning on MOFâ€Đerived Catalysts. Small, 2022, 18, e2200720.	10.0	15
18	Revealing the Structure–Interaction–Dissolubility Relationships through Computational Investigation Coupled with Solubility Measurement: Toward Solvent Design for Organosulfide Capture. Industrial & Engineering Chemistry Research, 2022, 61, 7183-7192.	3.7	7

#	Article	IF	CITATIONS
19	Gas Diffusion Layer with a Regular Hydrophilic Structure Boosts the Power Density of Proton Exchange Membrane Fuel Cells via the Construction of Water Highways. ACS Applied Materials & Interfaces, 2022, 14, 17578-17584.	8.0	6
20	Enhancing electrocatalytic <scp>N<sub>2</sub></scp> reduction via tailoring the electric double layers. AICHE Journal, 2022, 68, .	3.6	17
21	Photoassisted Cobalt-Catalyzed Asymmetric Reductive Grignard-Type Addition of Aryl Iodides. Journal of the American Chemical Society, 2022, 144, 8347-8354.	13.7	52
22	Programmable protein topology via <scp>SpyCatcherâ€6pyTag</scp> chemistry in oneâ€pot cellâ€free expression system. Protein Science, 2022, 31, .	7.6	5
23	Asymmetric pore windows in MOF membranes for natural gas valorization. Nature, 2022, 606, 706-712.	27.8	163
24	Edge-enriched MoS2@C/rGO film as self-standing anodes for high-capacity and long-life lithium-ion batteries. Science China Materials, 2021, 64, 96-104.	6.3	30
25	Pt1.4Ni(100) Tetrapods with Enhanced Oxygen Reduction Reaction Activity. Catalysis Letters, 2021, 151, 212-220.	2.6	7
26	Highâ€damping polyurethane/hollow glass microspheres sound insulation materials: Preparation and characterization. Journal of Applied Polymer Science, 2021, 138, 49970.	2.6	23
27	Supersaturated bridge-sulfur and vanadium co-doped MOS2 nanosheet arrays with enhanced sodium storage capability. Nano Research, 2021, 14, 74-80.	10.4	42
28	Fluorination-enabled Reconstruction of NiFe Electrocatalysts for Efficient Water Oxidation. Nano Letters, 2021, 21, 492-499.	9.1	190
29	Pyruvate Kinase M2 Mediates Glycolysis in the Lymphatic Endothelial Cells and Promotes the Progression of Lymphatic Malformations. American Journal of Pathology, 2021, 191, 204-215.	3.8	11
30	Atomic heterointerface engineering overcomes the activity limitation of electrocatalysts and promises highly-efficient alkaline water splitting. Energy and Environmental Science, 2021, 14, 5228-5259.	30.8	198
31	Surface covalent sulfur enriching Ni active sites of Ni <sub>3</sub> S <sub>2</sub> nanoparticles for efficient oxygen evolution. New Journal of Chemistry, 2021, 45, 3210-3214.	2.8	5
32	A reticular chemistry guide for the design of periodic solids. Nature Reviews Materials, 2021, 6, 466-487.	48.7	166
33	Multivalent Ion Batteries: Cathode Design for Aqueous Rechargeable Multivalent Ion Batteries: Challenges and Opportunities (Adv. Funct. Mater. 13/2021). Advanced Functional Materials, 2021, 31, 2170089.	14.9	1
34	Derived CuSn Alloys from Heterointerfaces in Bimetallic Oxides Promote the CO <sub>2</sub> Electroreduction to Formate. ChemElectroChem, 2021, 8, 1150-1155.	3.4	11
35	BiPO <sub>4</sub> â€Đerived 2D Nanosheets for Efficient Electrocatalytic Reduction of CO <sub>2</sub> to Liquid Fuel. Angewandte Chemie, 2021, 133, 7759-7763.	2.0	10
36	BiPO <sub>4</sub> â€Derived 2D Nanosheets for Efficient Electrocatalytic Reduction of CO <sub>2</sub> to Liquid Fuel. Angewandte Chemie - International Edition, 2021, 60, 7681-7685.	13.8	98

#	Article	IF	CITATIONS
37	Multivalence-Ion Intercalation Enables Ultrahigh 1T Phase MoS <sub>2</sub> Nanoflowers to Enhanced Sodium-Storage Performance. CCS Chemistry, 2021, 3, 1472-1482.	7.8	26
38	Revealing the Sudden Alternation in Pt@hâ€BN Nanoreactors for Nearly 100% CO <sub>2</sub> â€ŧo H <sub>4</sub> Photoreduction. Advanced Functional Materials, 2021, 31, 2010780.	14.9	43
39	Surface enrichment and diffusion enabling gradient-doping and coating of Ni-rich cathode toward Li-ion batteries. Nature Communications, 2021, 12, 4564.	12.8	153
40	New insights on ultrafast Na[solv]+ coinserted graphite driven by an electric field. Science China Materials, 2021, 64, 2967-2975.	6.3	3
41	Facile Fabrication of Robust Hydrogen Evolution Electrodes under High Current Densities via Pt@Cu Interactions. Advanced Functional Materials, 2021, 31, 2105579.	14.9	45
42	Cathode Design for Aqueous Rechargeable Multivalent Ion Batteries: Challenges and Opportunities. Advanced Functional Materials, 2021, 31, 2010445.	14.9	102
43	Structure–Property–Energetics Relationship of Organosulfide Capture Using Cu(I)/Cu(II)-BTC Edited by Valence Engineering. Industrial & Engineering Chemistry Research, 2021, 60, 371-377.	3.7	8
44	Integrated Reference Electrodes in Anion-Exchange-Membrane Electrolyzers: Impact of Stainless-Steel Gas-Diffusion Layers and Internal Mechanical Pressure. ACS Energy Letters, 2021, 6, 305-312.	17.4	63
45	Optimizing SnO <sub>2â^'</sub> <i><sub>x</sub></i> /Fe <sub>2</sub> O <sub>3</sub> Heteroâ€Nanocrystals Toward Rapid and Highly Reversible Lithium Storage. Small, 2021, 17, e2103532.	10.0	20
46	Lightâ€Motivated SnO <sub>2</sub> /TiO <sub>2</sub> Heterojunctions Enabling the Breakthrough in Energy Density for Lithiumâ€Ion Batteries. Advanced Materials, 2021, 33, e2103558.	21.0	73
47	RDFNet: A Fast Caries Detection Method Incorporating Transformer Mechanism. Computational and Mathematical Methods in Medicine, 2021, 2021, 1-9.	1.3	15
48	Computational fluid dynamics simulation and experimental analysis of ultrafine powder suspension. Rare Metals, 2020, 39, 850-860.	7.1	3
49	Positively charged Pt-based cocatalysts: an orientation for achieving efficient photocatalytic water splitting. Journal of Materials Chemistry A, 2020, 8, 17-26.	10.3	71
50	Enabling stable MnO <sub>2</sub> matrix for aqueous zinc-ion battery cathodes. Journal of Materials Chemistry A, 2020, 8, 22075-22082.	10.3	101
51	Introducing a Cantellation Strategy for the Design of Mesoporous Zeolite-like Metal–Organic Frameworks: Zr-sod-ZMOFs as a Case Study. Journal of the American Chemical Society, 2020, 142, 20547-20553.	13.7	31
52	Promoting CO2 methanation via ligand-stabilized metal oxide clusters as hydrogen-donating motifs. Nature Communications, 2020, 11, 6190.	12.8	93
53	A novel antiviral IncRNA, EDAL, shields a T309 O-GlcNAcylation site to promote EZH2 lysosomal degradation. Genome Biology, 2020, 21, 228.	8.8	38
54	Extension of Surface Organometallic Chemistry to Metal–Organic Frameworks: Development of a Well-Defined Single Site [(≡Zr–Oâ^')W(â•O)(CH <sub>2</sub> <sup><i>t</i></sup> Bu) <sub>3</sub> ] Olefi Metathesis Catalyst. Journal of the American Chemical Society, 2020, 142, 16690-16703.	n 13.7	31

#	Article	IF	CITATIONS
55	Intermediate Binding Control Using Metal–Organic Frameworks Enhances Electrochemical CO <sub>2</sub> Reduction. Journal of the American Chemical Society, 2020, 142, 21513-21521.	13.7	133
56	A fatigue damage accumulation model for reliability analysis of engine components under combined cycle loadings. Fatigue and Fracture of Engineering Materials and Structures, 2020, 43, 1880-1892.	3.4	36
57	Rich Bismuthâ€Oxygen Bonds in Bismuth Derivatives from Bi <sub>2</sub> S <sub>3</sub> Preâ€Catalysts Promote the Electrochemical Reduction of CO <sub>2</sub> . ChemElectroChem, 2020, 7, 2864-2868.	3.4	12
58	Nanospaceâ€Confinement Synthesis: Designing Highâ€Energy Anode Materials toward Ultrastable Lithiumâ€Ion Batteries. Small, 2020, 16, e2002351.	10.0	13
59	Reticular Chemistry 3.2: Typical Minimal Edge-Transitive <i>Derived</i> and <i>Related</i> Nets for the Design and Synthesis of Metal–Organic Frameworks. Chemical Reviews, 2020, 120, 8039-8065.	47.7	149
60	Aerosol Spray Pyrolysis Synthesis of Porous Anatase TiO2 Microspheres with Tailored Photocatalytic Activity. Acta Metallurgica Sinica (English Letters), 2019, 32, 286-296.	2.9	4
61	Gangliosides profiling in serum of breast cancer patient: GM3 as a potential diagnostic biomarker. Glycoconjugate Journal, 2019, 36, 419-428.	2.7	29
62	Unique holey graphene/carbon dots frameworks by microwave-initiated chain reduction for high-performance compressible supercapacitors and reusable oil/water separation. Journal of Materials Chemistry A, 2019, 7, 22054-22062.	10.3	27
63	Research progress in materials-oriented chemical engineering in China. Reviews in Chemical Engineering, 2019, 35, 917-927.	4.4	2
64	Revealing the Electrochemical Mechanism of Cationic/Anionic Redox on Li-Rich Layered Oxides via Controlling the Distribution of Primary Particle Size. ACS Applied Materials & Interfaces, 2019, 11, 25796-25803.	8.0	8
65	Continuous oxygen vacancy engineering of the Co <sub>3</sub> O <sub>4</sub> layer for an enhanced alkaline electrocatalytic hydrogen evolution reaction. Journal of Materials Chemistry A, 2019, 7, 13506-13510.	10.3	78
66	Comprehensive <i>N</i> -Glycome Profiling of Cells and Tissues for Breast Cancer Diagnosis. Journal of Proteome Research, 2019, 18, 2559-2570.	3.7	26
67	<i>110th Anniversary:</i> Concurrently Coating and Doping High-Valence Vanadium in Nickel-Rich Lithiated Oxides for High-Rate and Stable Lithium-Ion Batteries. Industrial & Engineering Chemistry Research, 2019, 58, 4108-4115.	3.7	33
68	Tailorable surface sulfur chemistry of mesoporous Ni <sub>3</sub> S <sub>2</sub> particles for efficient oxygen evolution. Journal of Materials Chemistry A, 2019, 7, 7548-7552.	10.3	72
69	Patterns of human social contact and contact with animals in Shanghai, China. Scientific Reports, 2019, 9, 15141.	3.3	61
70	Enriching the Reticular Chemistry Repertoire with Minimal Edge-Transitive Related Nets: Access to Highly Coordinated Metal–Organic Frameworks Based on Double Six-Membered Rings as Net-Coded Building Units. Journal of the American Chemical Society, 2019, 141, 20480-20489.	13.7	42
71	Extremely Hydrophobic POPs to Access Highly Porous Storage Media and Capturing Agent for Organic Vapors. CheM, 2019, 5, 180-191.	11.7	42
72	Optimized in vivo performance of acid-liable micelles for the treatment of rheumatoid arthritis by one single injection. Nano Research, 2019, 12, 421-428.	10.4	24

#	Article	IF	CITATIONS
73	Unsaturated Sulfur Edge Engineering of Strongly Coupled MoS <sub>2</sub> Nanosheet–Carbon Macroporous Hybrid Catalyst for Enhanced Hydrogen Generation. Advanced Energy Materials, 2019, 9, 1802553.	19.5	159
74	In-situ growth of ultrathin MoS2 nanosheets on sponge-like carbon nanospheres for lithium-ion batteries. Science China Materials, 2018, 61, 1049-1056.	6.3	20
75	Multi-shelled LiMn1.95Co0.05O4 cages with a tunable Mn oxidation state for ultra-high lithium storage. New Journal of Chemistry, 2018, 42, 3953-3960.	2.8	3
76	Turning the Old Adjuvant from Gel to Nanoparticles to Amplify CD8 <sup>+</sup> T Cell Responses. Advanced Science, 2018, 5, 1700426.	11.2	93
77	Nanospaceâ€confined synthesis of coconutâ€like SnS/C nanospheres for highâ€rate and stable lithiumâ€ion batteries. AICHE Journal, 2018, 64, 1965-1974.	3.6	45
78	2D Metal Chalcogenides Incorporated into Carbon and their Assembly for Energy Storage Applications. Small, 2018, 14, e1800148.	10.0	40
79	L1 <sub>2</sub> Atomic Ordered Substrate Enhanced Pt-Skin Cu <sub>3</sub> Pt Catalyst for Efficient Oxygen Reduction Reaction. ACS Applied Materials & Interfaces, 2018, 10, 38015-38023.	8.0	28
80	Construction of Nanoreactors Combining Two-Dimensional Hexagonal Boron Nitride (h-BN) Coating with Pt/Al <sub>2</sub> O <sub>3</sub> Catalyst toward Efficient Catalysis for CO Oxidation. Industrial & Engineering Chemistry Research, 2018, 57, 13353-13361.	3.7	13
81	Mo-Triggered amorphous Ni <sub>3</sub> S <sub>2</sub> nanosheets as efficient and durable electrocatalysts for water splitting. Materials Chemistry Frontiers, 2018, 2, 1462-1466.	5.9	43
82	Topology meets MOF chemistry for pore-aperture fine tuning: <b>ftw</b> -MOF platform for energy-efficient separations <i>via</i> adsorption kinetics or molecular sieving. Chemical Communications, 2018, 54, 6404-6407.	4.1	65
83	2D Nanospace Confined Synthesis of Pseudocapacitanceâ€Dominated MoS <sub>2</sub> â€inâ€īi <sub>3</sub> C <sub>2</sub> Superstructure for Ultrafast and Stable Li/Naâ€ion Batteries. Advanced Functional Materials, 2018, 28, 1804306.	14.9	194
84	Enriching the Reticular Chemistry Repertoire: Merged Nets Approach for the Rational Design of Intricate Mixed-Linker Metal–Organic Framework Platforms. Journal of the American Chemical Society, 2018, 140, 8858-8867.	13.7	129
85	3D Ordered Macroporous MoS <sub>2</sub> @C Nanostructure for Flexible Liâ€lon Batteries. Advanced Materials, 2017, 29, 1603020.	21.0	350
86	Tailoring polymeric hybrid micelles with lymph node targeting ability to improve the potency of cancer vaccines. Biomaterials, 2017, 122, 105-113.	11.4	107
87	Targeting NF-kB signaling with polymeric hybrid micelles that co-deliver siRNA and dexamethasone for arthritis therapy. Biomaterials, 2017, 122, 10-22.	11.4	161
88	Applying the Power of Reticular Chemistry to Finding the Missing alb-MOF Platform Based on the (6,12)-Coordinated Edge-Transitive Net. Journal of the American Chemical Society, 2017, 139, 3265-3274.	13.7	104
89	2D MoS <sub>2</sub> /polyaniline heterostructures with enlarged interlayer spacing for superior lithium and sodium storage. Journal of Materials Chemistry A, 2017, 5, 5383-5389.	10.3	102
90	Moâ€Based Ultrasmall Nanoparticles on Hierarchical Carbon Nanosheets for Superior Lithium Ion Storage and Hydrogen Generation Catalysis. Advanced Energy Materials, 2017, 7, 1602782.	19.5	123

HAO JIANG

#	Article	IF	CITATIONS
91	Isoreticular rare earth fcu-MOFs for the selective removal of H2S from CO2 containing gases. Chemical Engineering Journal, 2017, 324, 392-396.	12.7	98
92	Triosephosphate isomerase 1 suppresses growth, migration and invasion of hepatocellular carcinoma cells. Biochemical and Biophysical Research Communications, 2017, 482, 1048-1053.	2.1	44
93	Minimal edge-transitive nets for the design and construction of metal–organic frameworks. Faraday Discussions, 2017, 201, 127-143.	3.2	32
94	Lymph node targeting strategies to improve vaccination efficacy. Journal of Controlled Release, 2017, 267, 47-56.	9.9	207
95	Valuing Metal–Organic Frameworks for Postcombustion Carbon Capture: A Benchmark Study for Evaluating Physical Adsorbents. Advanced Materials, 2017, 29, 1702953.	21.0	88
96	Metal–Organic Framework-Based Separators for Enhancing Li–S Battery Stability: Mechanism of Mitigating Polysulfide Diffusion. ACS Energy Letters, 2017, 2, 2362-2367.	17.4	229
97	Kirigami-patterned highly stretchable conductors from flexible carbon nanotube-embedded polymer films. Journal of Materials Chemistry C, 2017, 5, 8714-8722.	5.5	63
98	Engineering the outermost layers of TiO <sub>2</sub> nanoparticles using <i>in situ</i> Mg doping in a flame aerosol reactor. AICHE Journal, 2017, 63, 870-880.	3.6	21
99	Dietary Keratan Sulfate from Shark Cartilage Modulates Gut Microbiota and Increases the Abundance of Lactobacillus spp Marine Drugs, 2016, 14, 224.	4.6	29
100	Homologous V <sub>2</sub> O <sub>3</sub> /C box-in-box and V <sub>2</sub> O <sub>5</sub> box for lithium-ion full cells. Journal of Materials Chemistry A, 2016, 4, 12030-12035.	10.3	39
101	Targeted delivery of low-dose dexamethasone using PCL–PEG micelles for effective treatment of rheumatoid arthritis. Journal of Controlled Release, 2016, 230, 64-72.	9.9	171
102	EZH2 is required for mouse oocyte meiotic maturation by interacting with and stabilizing spindle assembly checkpoint protein BubRI. Nucleic Acids Research, 2016, 44, 7659-7672.	14.5	25
103	A screening analysis of the GJB2 c.176 del 16 mutation responsible for hereditary deafness in a Chinese family. Journal of Otology, 2016, 11, 134-137.	1.0	2
104	Mosaic structure effect and superior catalytic performance of AgBr/Ag <sub>2</sub> MoO <sub>4</sub> composite materials. RSC Advances, 2016, 6, 94771-94779.	3.6	13
105	Confined Synthesis of FeS <sub>2</sub> Nanoparticles Encapsulated in Carbon Nanotube Hybrids for Ultrastable Lithium-Ion Batteries. ACS Sustainable Chemistry and Engineering, 2016, 4, 4251-4255.	6.7	126
106	CsPbBr <sub>3</sub> Perovskite Quantum Dots-Based Monolithic Electrospun Fiber Membrane as an Ultrastable and Ultrasensitive Fluorescent Sensor in Aqueous Medium. Journal of Physical Chemistry Letters, 2016, 7, 4253-4258.	4.6	137
107	Salt-Templating Protocol To Realize Few-Layered Ultrasmall MoS <sub>2</sub> Nanosheets Inlayed into Carbon Frameworks for Superior Lithium-Ion Batteries. ACS Sustainable Chemistry and Engineering, 2016, 4, 1148-1153.	6.7	39
108	Aerosol construction of multi-shelled LiMn <sub>2</sub> O <sub>4</sub> hollow microspheres as a cathode in lithium ion batteries. New Journal of Chemistry, 2016, 40, 1839-1844.	2.8	19

#	Article	IF	CITATIONS
109	Batteries: 2D Monolayer MoS <sub>2</sub> –Carbon Interoverlapped Superstructure: Engineering Ideal Atomic Interface for Lithium Ion Storage (Adv. Mater. 24/2015). Advanced Materials, 2015, 27, 3582-3582.	21.0	6
110	Faceâ€ŧoâ€Face Contact and Openâ€Void Coinvolved Si/C Nanohybrids Lithiumâ€Ion Battery Anodes with Extremely Long Cycle Life. Advanced Functional Materials, 2015, 25, 5395-5401.	14.9	85
111	Ultraâ€Tuning of the Rareâ€Earth fcuâ€MOF Aperture Size for Selective Molecular Exclusion of Branched Paraffins. Angewandte Chemie - International Edition, 2015, 54, 14353-14358.	13.8	222
112	2D Monolayer MoS <sub>2</sub> –Carbon Interoverlapped Superstructure: Engineering Ideal Atomic Interface for Lithium Ion Storage. Advanced Materials, 2015, 27, 3687-3695.	21.0	504
113	A graphene/carbon nanotube@ï€-conjugated polymer nanocomposite for high-performance organic supercapacitor electrodes. Journal of Materials Chemistry A, 2015, 3, 3880-3890.	10.3	58
114	Cationic micelle delivery of Trp2 peptide for efficient lymphatic draining and enhanced cytotoxic T-lymphocyte responses. Journal of Controlled Release, 2015, 200, 1-12.	9.9	84
115	One-step synthesis of SnO <sub>x</sub> nanocrystalline aggregates encapsulated by amorphous TiO <sub>2</sub> as an anode in Li-ion battery. Journal of Materials Chemistry A, 2015, 3, 9982-9988.	10.3	36
116	Ultrafine V <sub>2</sub> O <sub>3</sub> Nanowire Embedded in Carbon Hybrids with Enhanced Lithium Storage Capability. Industrial & Engineering Chemistry Research, 2015, 54, 2960-2965.	3.7	54
117	Tunable Rare Earth <b>fcu</b> -MOF Platform: Access to Adsorption Kinetics Driven Gas/Vapor Separations via Pore Size Contraction. Journal of the American Chemical Society, 2015, 137, 5034-5040.	13.7	308
118	Ultrathin MnO <sub>2</sub> nanoflakes grown on N-doped carbon nanoboxes for high-energy asymmetric supercapacitors. Journal of Materials Chemistry A, 2015, 3, 21337-21342.	10.3	66
119	Sn@Ni <sub>3</sub> Sn <sub>4</sub> embedded nanocable-like carbon hybrids for stable lithium-ion batteries. Chemical Communications, 2015, 51, 16373-16376.	4.1	19
120	Intracellular redox potential-responsive micelles based on polyethylenimine-cystamine-poly(ε-caprolactone) block copolymer for enhanced miR-34a delivery. Polymer Chemistry, 2015, 6, 1952-1960.	3.9	37
121	Hollow LiMn <sub>2</sub> O <sub>4</sub> Nanocones as Superior Cathode Materials for Lithiumâ€lon Batteries with Enhanced Power and Cycle Performances. Small, 2014, 10, 1096-1100.	10.0	63
122	Synthesis, microstructure evolution, and mechanical properties of (Cr <sub>1–<i>x</i></sub> V <sub><i>x</i></sub> ) <sub>2</sub> AlC ceramics by in situ hot-pressing method. Journal of Materials Research, 2014, 29, 1168-1174.	2.6	5
123	Graphene supported mesoporous single crystal silicon on Cu foam as a stable lithium-ion battery anode. Journal of Materials Chemistry A, 2014, 2, 16360-16364.	10.3	36
124	Self-assembling few-layer MoS <sub>2</sub> nanosheets on a CNT backbone for high-rate and long-life lithium-ion batteries. RSC Advances, 2014, 4, 40368-40372.	3.6	35
125	Highly compressible magnetic liquid marbles assembled from hydrophobic magnetic chain-like nanoparticles. RSC Advances, 2014, 4, 3162-3164.	3.6	20
126	SnO2 nanorod@TiO2 hybrid material for dye-sensitized solar cells. Journal of Materials Chemistry A, 2014, 2, 8266-8272.	10.3	40

HAO JIANG

#	Article	IF	CITATIONS
127	Rational Design of MnO/Carbon Nanopeapods with Internal Void Space for High-Rate and Long-Life Li-Ion Batteries. ACS Nano, 2014, 8, 6038-6046.	14.6	420
128	Highly Stretchable Conductors Integrated with a Conductive Carbon Nanotube/Graphene Network and 3D Porous Poly(dimethylsiloxane). Advanced Functional Materials, 2014, 24, 7548-7556.	14.9	162
129	Nanostructured Ternary Nanocomposite of rGO/CNTs/MnO <sub>2</sub> for High-Rate Supercapacitors. ACS Sustainable Chemistry and Engineering, 2014, 2, 70-74.	6.7	102
130	Assembly and copper ions detection of highly sensible and stable hydroxyapatite nanocomposite fluorescence probe. Micro and Nano Letters, 2014, 9, 127-131.	1.3	5
131	Hydrothermal synthesis of hollow Mn2O3 nanocones as anode material for Li-ion batteries. RSC Advances, 2013, 3, 19778.	3.6	58
132	Phase-segregation induced growth of core–shell α-Fe2O3/SnO2 heterostructures for lithium-ion battery. CrystEngComm, 2013, 15, 6715.	2.6	27
133	In situ Au-catalyzed fabrication of branch-type SnO2 nanowires by a continuous gas-phase route for dye-sensitized solar cells. Journal of Materials Chemistry A, 2013, 1, 13814.	10.3	16
134	Construction of core–shell Fe2O3@SnO2 nanohybrids for gas sensors by a simple flame-assisted spray process. RSC Advances, 2013, 3, 22373.	3.6	21
135	3D carbon based nanostructures for advanced supercapacitors. Energy and Environmental Science, 2013, 6, 41-53.	30.8	1,389
136	Functional mesoporous carbon-coated CNT network for high-performance supercapacitors. New Journal of Chemistry, 2013, 37, 1294.	2.8	12
137	Mixed Solvents Assisted Flame Spray Pyrolysis Synthesis of TiO <sub>2</sub> Hierarchically Porous Hollow Spheres for Dye-Sensitized Solar Cells. Industrial & Engineering Chemistry Research, 2013, 52, 11029-11035.	3.7	32
138	A Novel Ohmic-Loss Reduction Control Strategy for Planar Motor. IEEE Transactions on Magnetics, 2012, 48, 2997-3000.	2.1	2
139	Hierarchical porous nanostructures assembled from ultrathin MnO <sub>2</sub> nanoflakes with enhanced supercapacitive performances. Journal of Materials Chemistry, 2012, 22, 2751-2756.	6.7	135
140	A green and high energy density asymmetric supercapacitor based on ultrathin MnO <sub>2</sub> nanostructures and functional mesoporous carbon nanotube electrodes. Nanoscale, 2012, 4, 807-812.	5.6	276
141	Hierarchical porous NiCo2O4 nanowires for high-rate supercapacitors. Chemical Communications, 2012, 48, 4465.	4.1	544
142	High-performance supercapacitor material based on Ni(OH)2 nanowire-MnO2 nanoflakes core–shell nanostructures. Chemical Communications, 2012, 48, 2606.	4.1	244
143	Stable Core Shell Co <sub>3</sub> Fe <sub>7</sub> –CoFe <sub>2</sub> O <sub>4</sub> Nanoparticles Synthesized via Flame Spray Pyrolysis Approach. Industrial & Engineering Chemistry Research, 2012, 51, 11157-11162.	3.7	35
144	Polyaniline–MnO2 coaxial nanofiber with hierarchical structure for high-performance supercapacitors. Journal of Materials Chemistry, 2012, 22, 16939.	6.7	157

#	Article	IF	CITATIONS
145	Mesoporous Carbon Incorporated Metal Oxide Nanomaterials as Supercapacitor Electrodes. Advanced Materials, 2012, 24, 4197-4202.	21.0	548

## 146 Mesoporous Carbon Incorporated Metal Oxide Nanomaterials as Supercapacitor Electrodes (Adv.) Tj ETQq0 0 0 rgBT / Overlock 10 Tf 50

147	Functional mesoporous carbon nanotubes and their integration in situ with metal nanocrystals for enhanced electrochemical performances. Chemical Communications, 2011, 47, 8590.	4.1	66
148	Peapod-like nickel@mesoporous carbon core-shell nanowires: a novel electrode material for supercapacitors. RSC Advances, 2011, 1, 954.	3.6	45
149	High–rate electrochemical capacitors from highly graphitic carbon–tipped manganese oxide/mesoporous carbon/manganese oxide hybrid nanowires. Energy and Environmental Science, 2011, 4, 1813.	30.8	315
150	Magnetic fields study of various planar Halbach permanent magnet array. , 2010, , .		1
151	Calculation and investigation of end-effect for a high-precision planar magnetic levitation. , 2010, , .		0
152	Design and analysis of a novel ironless trapezoid winding array with single-sided and well sinusoidal magnetic field. , 2010, , .		1
153	Large-scale, uniform, single-crystalline Cd(OH)2 hexagonal platelets for Cd-based functional applications. CrystEngComm, 2010, 12, 1726.	2.6	15
154	Uniform, thin and continuous graphitic carbon tubular coatings on CdS nanowires. Journal of Materials Chemistry, 2009, 19, 1093.	6.7	7
155	Rectangular or square, tapered, and single-crystal PbTe nanotubes. Journal of Materials Chemistry, 2009, 19, 3063.	6.7	12
156	Hydrothermal synthesis of novel In2O3 microspheres for gas sensors. Chemical Communications, 2009, , 3618.	4.1	41
157	ZnO–Si side-to-side biaxial nanowire heterostructures with improved luminescence. Journal of Materials Chemistry, 2009, 19, 7011.	6.7	12
158	Stable field emission performance from urchin-like ZnO nanostructures. Nanotechnology, 2009, 20, 055706.	2.6	40